Nicotine Increases the VEGF/PEDF Ratio in Retinal Pigment Epithelium: A Possible Mechanism for CNV in Passive Smokers with AMD

Marianne Pons and Maria E. Marin-Castaño

Purpose. Cigarette smoking is the strongest environmental risk factor for wet age-related macular degeneration (AMD). Inappropriate expression of proangiogenic vascular endothelial growth factor (VEGF) and antiangiogenic pigment epithelium derived factor (PEDF) may cause choroidal neovascularization (CNV), a key event in wet AMD, resulting in vision loss. Nicotine (NT), a potent angiogenic agent abundant in second-hand smoke, may play a major role in the pathogenesis of wet AMD. The purpose of this study was to evaluate the expression of nicotinic acetylcholine receptors (nAchR) in retinal pigment epithelium (RPE) and determine the effects of NT on RPE-derived VEGF and PEDF expression in the context of passive smoking.

Methods. Human RPE cells were treated with NT (10^{-8} M), with or without the nAchR-nonspecific antagonist hexamethonium (HXM) (10^{-5} M) for 72 hours. RPE sheets were microdissected from rats exposed to NT in drinking water (100 μg/mL), with or without HXM (40 mg/kg/d, intraperitoneally), for 72 hours. Cell death was determined by cell count and proliferation by Western blot for proliferating cell nuclear antigen (PCNA). nAchR expression was examined by real-time PCR and Western blot. ERK activation was evaluated by Western blot analysis. VEGF and PEDF expression was assessed by ELISA, Western blot, and real-time PCR.

Results. Cultured RPE cells constitutively expressed the nAchR α3, α10, and β1 subunits, with β1 being the most prevalent. The nAchR α4, α5, α7, and β2 subunits were detected in RPE sheets from rats, among which α4 is the predominant subtype. NT, which did not result in either cell death or proliferation, induced β1 nAchR, upregulated VEGF, and downregulated PEDF expression through nAChR in ARPE-19 cells. Transcriptional activation of the nAchR α4 subunit and nAChR-mediated upregulation of VEGF and PEDF were observed in RPE from rats exposed to NT.

Conclusions. NT increased the VEGF-to-PEDF ratio in the RPE through nAchR in vitro and in vivo. This alteration in the ratio may play a key role in the progression to wet AMD in passive smokers. (*Invest Ophthalmol Vis Sci.* 2011;52:3842–3853) DOI:10.1167/iovs.10-6254

From the Bascom Palmer Eye Institute, Department of Ophthalmology, University of Miami Miller School of Medicine, Miami, Florida.

Supported by Flight Attendant Medical Research Institute Grant 072100_CIA; an unrestricted grant from Research to Prevent Blindness to the University of Miami; and National Institutes of Health Grant P30-EY14801.

Submitted for publication July 20, 2010; revised August 31, October 8, and December 23, 2010; accepted January 19, 2011.

Disclosure: **M. Pons**, None; **M.E. Marin-Castaño**, None

Corresponding author: Maria E. Marin-Castaño, Bascom Palmer Eye Institute, University of Miami Miller School of Medicine, 1638 NW 10th Avenue, Miami, FL, 33136; mcastano@med.miami.edu.

Age-related macular degeneration (AMD), a degenerative disease of the retina, is the leading cause of blindness in the elderly worldwide and has devastating effects on an individual's quality of life.[1–4] As older people make up the fastest growing segment of the population, AMD is becoming a serious public health issue. AMD affects more than 1.75 million individuals in the United States, and it is estimated that more than 300,000 new cases are diagnosed annually.[1,3] Unless better preventive treatments emerge, this number is expected to climb and even to reach epidemic proportions with the overall aging demographics.[5] Currently, there is no cure for AMD, and treatments are very limited.

AMD occurs in two main forms: dry and neovascular, or wet.[6] Only a fraction of patients with dry AMD develop the wet form of the disease, the most aggressive type of the condition, which accounts for 80% to 90% of cases of severe vision loss related to AMD. Choroidal neovascularization (CNV) is a key event in wet AMD, characterized by the growth of abnormal blood vessels that originate from the choroid through defects in Bruch's membrane and invade the region beneath the retinal pigment epithelium (RPE). CNV can cause bleeding and fluid leakage, which, along with RPE and photoreceptor destruction, lead to rapid vision loss if left untreated. Although our understanding of the two forms has increased substantially, there is still much debate as to why and how the disease progresses and what elements lead to the progression from dry to wet AMD.

A shift in the delicate balance between angiogenic stimulators and inhibitors may be involved in the development of CNV.[7] Vascular endothelial growth factor (VEGF) is a major angiogenic cytokine central in the development of wet AMD,[8–10] whereas the potent angiogenic inhibitor pigment epithelium-derived factor (PEDF) counterbalances the effect of VEGF.[11,12] The RPE, which supports photoreceptor cell function and plays a pivotal role in the maintenance of the outer retina, is recognized as the initial pathogenic target in AMD.[13] In the healthy eye, the RPE secretes a variety of growth factors, including VEGF[14] and PEDF.[15] Although the initiation of CNV is not well understood, the dysregulated expression of VEGF and PEDF by RPE cells may be involved.[16]

Although the pathophysiological mechanisms that cause AMD are not well understood, this multifactorial degenerative disease clearly results from a complex interplay among genetic[17] and environmental risk factors, among which cigarette smoking is the single most important preventable factor.[18–21] Overwhelming evidence shows that smokers have a greater prevalence of AMD than do nonsmokers,[18,19,22–27] and former smokers remain at high risk for AMD.[25] Although Khan et al.[28] reported that passive smoking almost doubles the risk of AMD,[28] data with regard to the possible link between passive smoking and AMD are scarce and often conflicting.[29] Passive smoking, also known as second-hand smoke or environmental tobacco exposure is the combination of mainstream smoke exhaled by the smoker and sidestream smoke that comes from

the burning end of a cigarette. Apart from active cigarette smoking, SHS, a toxic cocktail consisting of more than 4000 chemical compounds, is a widespread source of nicotine (NT) exposure,[30,31] as it contains twice as much NT per unit volume as does smoke inhaled from a cigarette. NT is not only the major bioactive and addictive component of cigarette smoke, but also is a potent angiogenic agent.[32,33] NT exerts its biological effects through binding to nicotinic cholinergic receptors (nAchR),[34,35] which are expressed in a variety of peripheral non-neuronal cells.[36–44] Although several nAChR subtypes have been reported in human choroidal and retinal endothelial cells,[41] the presence of nAchR in the RPE has not been investigated. Our group has shown that NT increases the size and severity of experimental CNV in mice.[45] NT promotes angiogenic tube formation in vitro in choroidal and retinal endothelial cells.[41] A recent study showed that the proangiogenic effect of NT is mediated by the α7 nAchR in human retinal endothelial cells.[46] It has also been reported that activation of nAChR by NT may contribute to the increased incidence of CNV seen in smokers with AMD.[41] The angiogenic activity of nAchR and its implication in tobacco-related vascular diseases have been discussed in a review published by Egleton et al.[47] Furthermore, NT upregulates the expression of VEGF in endothelial cells[48] and induces endothelial cell proliferation.[32,33,43] It is thus likely that NT promotes the pathologic angiogenesis seen in CNV and therefore plays a key role in the pathogenesis of wet AMD. We and others have shown that cigarette smoke and hydroquinone, a major pro-oxidant in cigarette smoke, cause oxidative damage to the RPE that may be critical in the pathogenesis of dry AMD.[49–54] To our knowledge, no study has ever been conducted on NT, passive smoking, and angiogenesis in the RPE. Therefore, the purpose of this study, which combined the simplicity of an in vitro approach and the complexity of an animal model, was to characterize the contribution of the RPE to the proangiogenic effects of NT in the context of passive smoking. The results presented may help explain the progression of AMD toward CNV in individuals who are passive smokers.

Material and Methods

Cell Culture

ARPE-19 cells, a nontransformed human RPE cell line[55] obtained from American Type Culture Collection (Manassas, VA), were grown to confluence in Dulbecco's modified Eagle's medium-Ham's F12 (DMEM/F12; 1:1 vol/vol) growth medium supplemented with 10% fetal bovine serum (FBS), 1 mM L-glutamine, 100 μg/mL penicillin/streptomycin, and 0.348% Na_2CO_3 (Invitrogen-Gibco Carlsbad, CA) in a 5% CO_2 humidified air incubator at 37°C. For the experiments, the cells were divided and plated at subconfluent density in six-well plates and grown to confluence. At the time of confluence, the medium was replaced for 24 hours with phenol red–free medium supplemented with 10% FBS. The cells were then treated in phenol red–free 1% FBS medium with NT 10^{-8} M (Sigma-Aldrich, St. Louis, MO) for various times. In some experiments, the cells were pretreated for 1 hour with the nonspecific nicotinic antagonist hexamethonium chloride (HXM; 10^{-5} M; Sigma-Aldrich) before they were treated with NT 10^{-8} M for 10 minutes or 72 hours. After treatment, the cells were washed with phosphate-buffered saline and harvested for protein with a lysis buffer (M-PER; Pierce, Rockford, IL) or RNA extraction (TRI reagent; Sigma-Aldrich). All experiments (triplicate wells for each condition) were performed at least in triplicate. The number of surviving cells was measured by cell count at the end of the treatment with NT (model Z1 particle counter; Beckman Coulter, Hialeah, FL).

Animals

Nine-month-old male Sprague-Dawley rats were obtained from Jackson Laboratories (Bar Harbor, ME) and maintained at the McKnight Vision Research Center at the University of Miami Miller School of Medicine, in compliance with institutional regulations. This study was conducted according to the ARVO Statement for the Use of Animals in Ophthalmic and Vision Research and was approved by the University of Miami Care and Use Committee. The experiments were performed in accordance with the Animal Welfare Act provisions and all other animal welfare guidelines for the care and use of laboratory animals. The rats were randomly divided into four groups (n = 5, each group):

Group 1: control rats receiving unaltered drinking tap water.

Group 2: rats receiving NT orally in drinking water (100 μg/mL) for 3 days.

Group 3: rats receiving unaltered drinking tap water and HXM chloride by daily intraperitoneal injection (40 mg/kg/d) for 3 days;

Group 4: rats receiving NT orally in drinking water in combination with HXM chloride by intraperitoneal injection for 3 days.

The definition of passive smoking varies considerably from study to study.[29] Most cigarettes contain 0.5 to 1.63 mg of NT per cigarette in the mainstream smoke (environmental tobacco exposure) exhaled by the smoker.[56] Herein, NT was administered at a dose of 100 μg/mL to simulate passive smoking, as the overall intake of NT was predicted to range between 3.0 and 3.6 mg (equivalent to six cigarettes) based on a daily water intake of 30 to 36 mL/rat. The rats were housed in plastic cages with free access to food and water, and were kept on a 12-hour light–dark cycle.

Human Primary RPE Cell Line

One pair of eyes (84-year-old female donor) not suitable for transplantation was obtained from the Lions Eye Bank (Miami, FL). The eyes were rinsed twice with 10% gentamicin and then washed in DMEM followed by an enzymatic digestion in 2% Dispase in DMEM for 45 minutes at 37°C. They were then washed twice in growth medium and subsequently transferred into fresh growth medium for microdissection. Using an upright dissection microscope, the anterior segment was removed, and the vitreous-retina was separated from the RPE and choroid. The RPE monolayer was dissected from Bruch's membrane, and the choroid and intact sheets of RPE cells were peeled and collected in a 15-mL tube. The RPE cells were centrifuged at 1500 rpm for 5 minutes and resuspended in growth medium. The cell suspension (0.5 mL/well) was added to a 12-well plate containing growth medium. They were cultured at 37°C in 5% CO_2 for 10 days, with the medium changed every other day. After 10 days, the cells were trypsinized, collected in a tube, centrifuged at 1000 rpm for 5 minutes, and resuspended in growth medium. They were then plated in six-well plates until confluence was reached, at which time they were trypsinized and grown in a larger flask. The identity of the cultured RPE cells was confirmed by positive staining for cytokeratin 8 and 18 (a kind gift from Boris Stanzel, University Eye Hospital Bonn, Germany) and ZO1 (Invitrogen-Gibco) (data not shown). Our management of the donor eyes adhered to the tenets of the Declaration of Helsinki for research involving human subjects.

Isolation of Rat RPE Sheets

At the end of the experimental period, rats were euthanized with CO_2, and the eyes were immediately removed and microdissected for recovery of RPE sheets as described above. Total protein and RNA were extracted and stored at −80°C.

Western Blot Analysis

Total protein was extracted from RPE cell lysates and RPE microdissected from rats exposed to NT for 3 days. Protein concentration was determined by a detergent-compatible protein assay (Bio-Rad, Hercules, CA). Thirty micrograms of protein were resolved on a 4% to 20% sodium dodecyl sulfate (SDS) polyacrylamide gel (Invitrogen) and transferred in 25 mM Tris, 192 mM glycine, 0.1% SDS, and 20% methanol (pH 8.4) to a nitrocellulose membrane (Hybond-ECL; GE Health care; Piscataway, NJ). Membranes were then blocked in Tris-

buffered saline (TBS)-Tween 20 buffer containing 5% nonfat dry milk (Bio-Rad, Hercules, CA) for 1 hour at room temperature. The blots were incubated overnight at 4°C with one of the following: mouse monoclonal phospho-ERK1/2, mouse monoclonal nAchR β1, mouse monoclonal PCNA (Santa Cruz Biotechnology Inc., Santa Cruz, CA), rabbit polyclonal ERK (Promega, Madison, WI), mouse monoclonal VEGF (Abcam, Cambridge, MA), mouse monoclonal PEDF (Chemicon Millipore, Billerica, MA), or rabbit monoclonal GAPDH (control to assure equal protein loading; Cell Signaling, Danvers, MA) antibody. The membranes were washed with TBS-Tween 20 and incubated with horseradish-peroxidase–linked donkey anti-rabbit or anti-mouse antibody (Santa Cruz Biotechnology Inc.) for 1 hour at room temperature. After final washes, immunofluorescence bands were detected by exposing the blots to a chemiluminescent solution (ECL Western Blot Substrate; Pierce) and then to autoradiograph film (Amersham Hyperfilm ECL; GE Health care). The bands were scanned and quantified by densitometry (ImageJ v1.34s software available by ftp at zippy.nimh-.nih.gov/ or at http://rsb.info.nih.gov/nih-imageJ; developed by Wayne Rasband, National Institutes of Health [NIH], Bethesda, MD).

Real-Time PCR

Total RNA was extracted (Tri reagent; Sigma-Aldrich) from RPE cells treated with NT 10^{-8} M and RPE microdissected from rats exposed to NT (100 μg/mL) for 3 days. RNA concentrations were measured spectrophotometrically (Nanodrop 2000; ThermoScientific, Waltham, MA), and the quality of each RNA sample was confirmed by calculating the ratio of optical density at 260:280 nm. Reverse transcription was performed with random primers on 1.25 μg of total RNA in a final reaction volume of 50 μL (High-Capacity cDNA Archive Kit; Applied Biosystems, Inc., Foster City, CA). Quantitative real-time PCR was performed (iCycler iQ system using iQ SybrGreen Supermix; Bio-Rad), as specified by the manufacturers' instructions, and the fluorescence thresholds were calculated with the system software. The primer sequences and size of the product for each targeted gene are described in Table 1. GAPDH was used as the endogenous control gene. Human GAPDH and VEGF primer sequences are available in the public domain RTPrimerDB database (http://medgen.UGent.be/rtprimerdb/).[57] Primer sequences for human PEDF, nAchR α3, α10 and β1 subunits are available in the qPrimerDepot database (http://primerdepot.nci.nih.gov/; NIH, Bethesda, MD). All primer sequences for rat GAPDH and VEGF[58]; PEDF[59]; and α4, α5, α7, and β2 nAchR[60] were previously published. Primers were purchased from Sigma-Aldrich. The amplification program consisted of 1 cycle at 95°C for 15 minutes, followed by 40 cycles at 95°C for 15 seconds, and 65°C for 1 minute. Regular PCR was performed with the primer sets, and the products were analyzed on an ethidium bromide–stained 2% agarose gel to confirm the product size and specificity (data not shown). Melting curves were also acquired and analyzed to ensure the specificity of the reaction. Each sample was run in duplicate and normalized to the GAPDH transcript content. The change ratio in mRNA levels was calculated using the $2^{-\Delta\Delta CT}$ method, with corrections for the housekeeping gene GAPDH.[61] Separate control experiments using serial dilutions of cDNA demonstrated that the efficiencies of each target gene and GAPDH amplification were similar, hence validating the use of comparative C_t method to determine relative expression of genes of interest (data not shown). To evaluate constitutive expression of nAchR subunits, real-time PCR products were visualized after electrophoresis separation on a 2% agarose gel. Pictures were captured using the molecular imager (ChemiDoc XRS system; Bio-Rad) for gel documentation.

ELISA for VEGF and PEDF

Cell supernatants were collected, and concentrations of VEGF (R&D Systems, Minneapolis, MN) and PEDF (Millipore Corp., Bedford, MA) were determined with an ELISA kit according to the manufacturer's instructions. Total protein content in the supernatant was also determined so that VEGF and PEDF expression could be calculated relative to total protein (nanograms/milligram of protein) and were subsequently expressed as a percentage of the control.

Statistical Analysis

Data expressed as a percentage of the control are the mean ± SEM of the results of three to six experiments performed in triplicate. Differences were analyzed using the nonparametric Kruskal-Wallis ANOVA with Dunn's multiple-comparison test and Student's *t*-test. $P < 0.05$ was considered statistically significant.

Results

Exposure to NT 10^{-8} M for 72 Hours Does Not Induce Either Cell Death or Proliferation in ARPE-19 Cells

The definition of passive smoking varies considerably from study to study.[29] However, reports show that concentrations of NT in the plasma of active smokers are higher than those found in the plasma of passive smokers. In a study published by our group in 2004, we investigated the effects of physiologic concentrations of NT comparable to those of active and passive smokers (10^{-6} and 10^{-8} M, respectively) on choroidal vascular smooth muscle cells.[45] Back in 1984, Benowitz et al.[62] showed

Table 1. Sequence of Real-Time PCR Primers

Target Gene	Forward Primer	Reverse Primer	Size (bp)
Human			
GAPDH	tgc acc acc aac tgc tta gc	ggc atg gac tgt ggt cat gag	87
VEGF	agg agg agg gca gaa tca tca	ctc gat tgg atg gca gta gct	76
PEDF	tcc aat gca gag gag tag ca	tgt gca ggc tta gag gga ct	93
α3 nAchR	ctt gct gct cac ctg gaa at	tat ggt ggg gca gag ttc at	102
α10 nAchR	gga cca cgt tgg tgc tg	cat ccc cag cag tct tgt gt	92
β1 nAchR	gca gca gca gga aca cag ta	ctc ttc tgg cca tct tcg tc	102
Rat			
GAPDH	atg gtg aag gtc ggt gtg	gaa ctt gcc gtg ggt aga g	82
VEGF	act gtg agc ctt gtt cag agc	cgg atc ttg gac aaa caa atg c	50
PEDF	aca ggg cag ctt ttg agt gg	atg aac ggt cgg tta agg tga ta	N/A
α4 nAchR	gga ccc tgg tga cta cga ga	cat aga aca ggt ggg cct tg	137
α5 nAchR	tgg aac acc tga gcg aca ag	cgt gac agt gcc gtt gta cc	284
α7 nAchR	aca ttg acg ttc gct ggt tc	cta cgg cgc atg gtt act gt	235
β2 nAchR	agc ctt ctt tgg ctg tgc tc	gag ccg tta gta gct gga cga	135

N/A, not available.

that NT plasma concentrations in active and passive smokers range between 10^{-6} and 10^{-8} M, respectively. Based on these observations, we elected to focus on NT 10^{-8} M, representative of the plasma concentration in passive smokers.

We first determined whether NT 10^{-8} M for 72 hours was the appropriate concentration and duration of exposure by assessing the number of surviving cells by cell count. We found that the number of cells after NT treatment was not different from control cells (Fig. 1A). Therefore, exposure to NT 10^{-8} M for 72 hours was not lethal in ARPE-19 cells.

NT has been shown to induce proliferation in a variety of cells including mesangial[44] and endothelial cells.[32,33,43] Therefore, the proliferative effects of NT were next examined by Western blot for PCNA, an endogenous marker of cell proliferation, on ARPE-19 cells exposed to NT 10^{-8} M for 72 hours. As shown in Figure 1B (left), addition of NT in concentrations reflecting those observed in the serum of passive smokers for three consecutive days did not upregulate PCNA protein expression in ARPE-19 cells, as shown by Western blot analysis.

To eliminate the possibility that the PCNA findings were due to the nonproliferative state of confluent cells, we next analyzed proliferation in response to NT in subconfluent ARPE-19 cells. Essentially the same results were achieved as those reported in confluent cells (Fig. 1B, right).

Human RPE Cells Constitutively Express the α3, α10, and β1 nAchR Subunits

NT exerts its biological effects through binding to nAChR.[34,35] nAchR is expressed in a variety of peripheral non-neuronal cells.[36–44] However, it is not known whether and which type of nAchR is expressed in human RPE cells. Therefore, to establish the presence of nAchR in RPE cells, we used real-time PCR to detect nAchR subtype transcripts in extracts from cultured ARPE-19 and primary RPE cells. As shown in Figures 2A, 2B, 2E, 2G, and 2H, we found that the nAChR α3, α10, and β1 subunits were expressed in the ARPE-19 cells. We did not detect significant expression of any other isoforms. The β1 nAchR subunit was by far the most abundant, as its expression was ~103-fold higher than that of α3 (103.7 ± 5.5 vs. 1.0 ± 0.03, $P < 0.0001$; Fig. 2A) and ~79-fold higher than α10 (79.5 ± 4.2 vs. 1.0 ± 0.07, $P < 0.0001$; Fig. 2B).

To exclude the possibility that our data collected in ARPE-19 cells may be an artifact due to the use of an immortalized cell line, nAchR expression was also evaluated by real-time PCR in a human primary RPE cell line generated and characterized in our laboratory (see the Material and Methods section). Indeed, similar results were achieved in ARPE-19 and primary RPE cells. We showed that primary RPE cells express the α3, α10, and β1 nAchR subunits (Figs. 2C, 2D, 2E, 2G, 2H). Levels of the β1 nAchR transcript were ~214-fold higher than α3 (215.2 ± 44.6 vs. 1.0 ± 0.05; $P < 0.001$; Fig. 2C) and ~52-fold higher than α10 (51.9 ± 10.8 vs. 1.0 ± 0.1, $P < 0.001$; Fig. 2D), thereby confirming that the nAchR β1 subtype is the most abundant isoform in RPE cells. To expand these findings, we used Western blot to confirm the presence of the β1 nAchR subtype in ARPE-19 and primary RPE cells. Consistent with the detection of mRNA encoding for the β1 nAchR subunit, both ARPE-19 and primary RPE cells constitutively expressed the β1 nAchR subtype (Fig. 2F). These findings demonstrate for the first time that human RPE cells constitutively express the nAchR α3, α10, and β1 subtypes, which could mediate the deleterious effects of NT on these cells. Based on the similarities between both cell lines, all subsequent experiments were conducted in ARPE-19 cells.

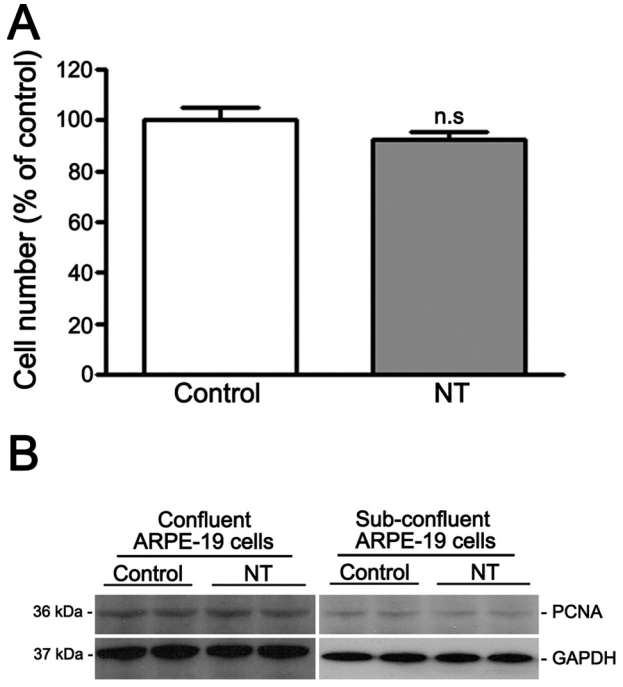

FIGURE 1. Effect of NT on ARPE-19 cells. (**A**) NT does not induce cell death. The number of surviving cells was determined by cell count in serum-starved confluent ARPE-19 cells exposed to NT 10^{-8} M for 72 hours. Data are expressed as a percentage of control and are the mean ± SE of three independent experiments run in duplicate. (**B**) NT does not induce cell proliferation. The proliferative effects of NT were examined by Western blot for PCNA on confluent (*left*) and subconfluent (*right*) serum-starved ARPE-19 cells exposed to NT 10^{-8} M for 72 hours. GAPDH served as the loading control. Shown is a Western blot from a representative experiment. The protein's molecular mass is shown at *left* in kilodaltons.

nAchRs Mediate NT-Induced ERK Phosphorylation in ARPE-19 Cells

To further investigate nAchR in RPE cells, we next postulated that these receptors were functional. NT has been shown to activate the ERK pathway in rat vascular smooth muscle cells.[63] To test the hypothesis and to characterize the signaling pathway by which NT exerts its effects on RPE cells, we next performed a time-course analysis of ERK phosphorylation by Western blot on cell lysates from ARPE-19 cells exposed to NT 10^{-8} M for various times (0, 1, 2, 5, 10, 20, and 30 minutes). As shown in Figure 3A, exposure of ARPE-19 cells to NT induced a rapid, robust, and sustained phosphorylation of ERK, starting as early as 1 minute, reaching a peak between 10 (466.6% ± 176.9% vs. 100.0% ± 0.97%; $P < 0.01$) and 20 (439.9% ± 177.4% vs. 100.0% ± 0.97%; $P < 0.05$) minutes, and declining quickly at 30 minutes (208.7% ± 13.10% vs. 100.0% ± 0.97%; $P < 0.01$). These observations demonstrate that the nAchRs expressed in cultured ARPE-19 cells are functional.

HXM is a broad-spectrum, nonspecific nAchR antagonist that blocks most heteromeric and homomeric forms of nAchR and provides a useful tool to explore the role of nAchR in biological processes. To confirm that NT-induced ERK phosphorylation was mediated by nAchR, we treated ARPE-19 cells with HXM 10^{-5} M for 1 hour before they were exposed to NT 10^{-8} M for 10 minutes. As presented in Figure 3B, HXM almost completely abolished NT-induced ERK phosphorylation in ARPE-19 cells (140.8 ± 29.8 vs. 496.6 ± 117.4, $P < 0.05$), establishing that ERK activation resulting from treatment with NT is mediated by nAchRs.

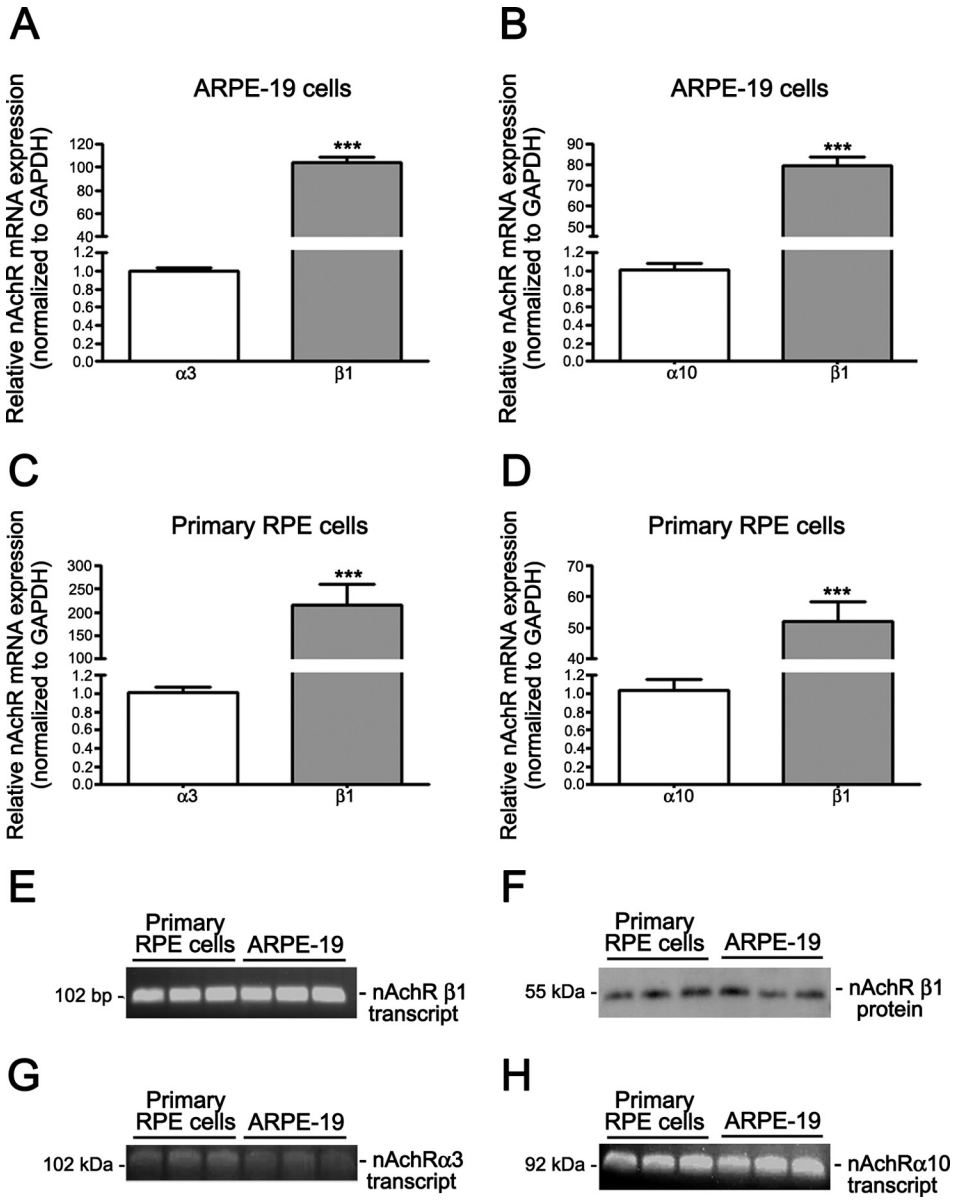

FIGURE 2. Human RPE cells constitutively expressed the $\alpha 3$, $\alpha 10$, and $\beta 1$ nAchR subunits. Real-time PCR demonstrated the presence of the nAchR $\alpha 3$, $\alpha 10$, and $\beta 1$ subunit transcripts and the prevalence of the $\beta 1$ subtype in confluent serum-starved (**A**, **B**, **E**, **G**, **H**) ARPE-19 and (**C**, **D**, **E**, **G**, **H**) human primary RPE cells. *GAPDH* was used as the housekeeping gene. Real-time PCR to determine the expression of the (**E**) $\beta 1$, (**G**) $\alpha 3$, and (**H**) $\alpha 10$ nAchRs was followed by ethidium bromide–stained agarose gel electrophoresis, to visualize the products in ARPE-19 and primary RPE cells. Shown are representative gels. At *left* is the size of the transcript in base pairs. (**F**) Western blot analysis demonstrated the expression of the most prevalent nAchR $\beta 1$ subunits in confluent, serum-starved ARPE-19 and primary RPE cells. Shown is a representative gel. The proteins' molecular mass is shown at the *left* in kilodaltons.

NT Induces the $\beta 1$ nAchR Subtype Transcriptional Activation in ARPE-19 Cells

Upregulation of brain nAChRs by chronic NT treatment has been reported in mice.[64] Herein, we investigated whether NT may modulate the $\beta 1$ nAchR subtype expression in RPE cells. The $\beta 1$nAchR isoform was our preferred target receptor because we found that it is the most abundant subtype in ARPE-19 cells. To address this question, we treated ARPE-19 cells with NT 10^{-8} M for 72 hours and $\beta 1$ nAchR subtype mRNA levels were determined by real-time PCR. As shown in Figure 4, expression of $\beta 1$ nAchR mRNA was increased by 39% (1.39 ± 0.04 vs. 1.00 ± 0.03, $P < 0.0001$) in response to NT compared with control cells. These observations suggest that chronic exposure to NT induces an upregulation of the number of $\beta 1$ nAchRs on the ARPE-19 cell surface.

NT Increases VEGF Expression and Decreases PEDF Expression through nAchR in ARPE-19 Cells

VEGF, produced and secreted by RPE cells in culture,[14] is a major angiogenic cytokine central to the development of wet AMD.[8–10] Therefore, we next determined the effect of NT on VEGF mRNA expression by real-time PCR. As shown in Figure 5A, we found that treatment with NT 10^{-8} M for 72 hours resulted in a robust ~82% increase in VEGF mRNA expression compared with control cells (1.82 ± 0.19 vs. 1.00 ± 0.02, $P < 0.0001$). VEGF protein released in the media by ARPE-19 cells in response to NT was increased by 27.3% relative to control cells as measured by ELISA (127.3% ± 5.4% vs. 100.0% ± 2.4%; $P < 0.001$; Fig. 5B).

PEDF, a potent angiogenic inhibitor,[15] counterbalances the effects of VEGF and modulates the formation of CNV.[65,66] Therefore, we next studied the effect of NT 10^{-8} M on PEDF mRNA expression by real-time PCR in ARPE-19 cells. As presented in Figure 5C, we found that treatment with NT for 72 hours led to a ~26% decrease in PEDF mRNA expression compared with that in control cells (0.74 ± 0.02 vs. 1.00 ± 0.05, $P < 0.0001$). The amount of PEDF protein secreted into the medium by ARPE-19 cells in response to NT was also decreased by ~28% compared with that in control cells (0.72% ± 9.1% versus 100.0% ± 4.2%, $P < 0.05$) as measured by ELISA (Fig. 5D). As a result of treatment with NT, the VEGF/PEDF protein ratio was increased by ~76% in ARPE-19 cells (1.76 ± 0.19 vs. 1.00 ± 0.02, $P < 0.05$; Fig. 5E).

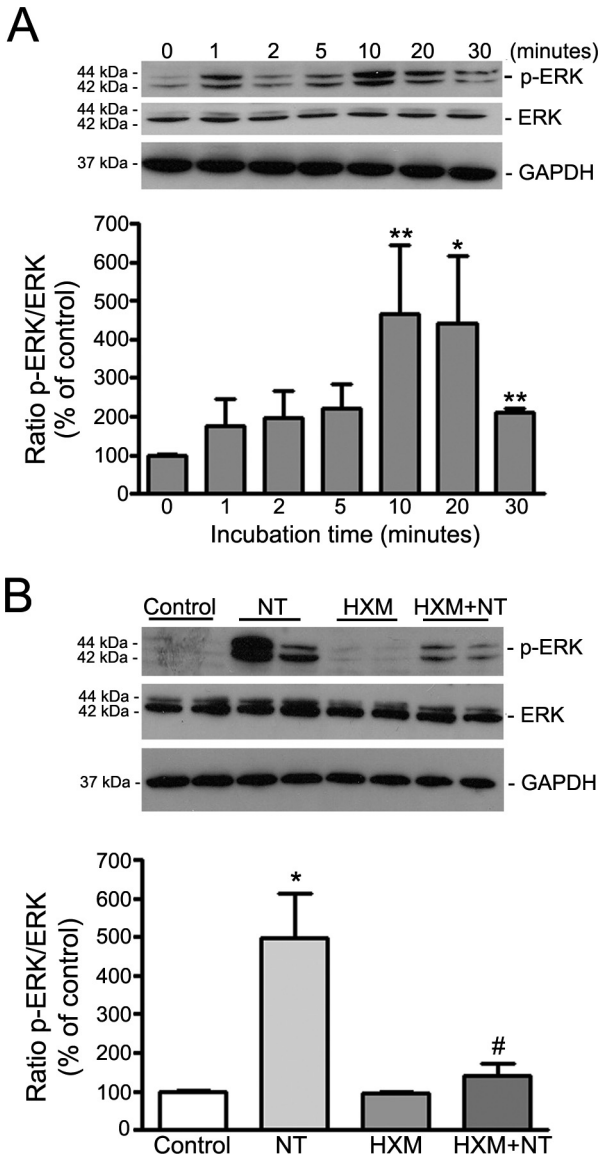

FIGURE 3. nAchRs mediated NT-induced ERK phosphorylation in ARPE-19 cells. (**A**) NT induced ERK phosphorylation in ARPE-19 cells. Total protein was extracted from confluent, serum-starved ARPE-19 cells incubated with NT 10^{-8} M for various times. (**B**) NT-induced ERK phosphorylation was prevented by the nonspecific nicotinic antagonist HXM. Total protein was extracted from serum-starved, confluent ARPE-19 cells preincubated with HXM 10^{-5} M for 1 hour then exposed to NT 10^{-8} M for 10 minutes. Phospho-ERK, total ERK, and GAPDH expression was assessed by Western blot analysis. *Top*: Western blot from a representative experiment. The proteins' molecular mass is shown at the *left* in kilodaltons. *Bottom:* average densitometry results of three independent experiments run in duplicate. p-ERK protein expression was normalized to total ERK. GAPDH served as loading control for ERK. Data are expressed as a percentage of control and are the mean ± SE of three independent experiments run in duplicate. $^{*}P < 0.05$ and $^{**}P < 0.01$ relative to control; $^{\#}P < 0.05$ relative to NT alone.

Next, we showed that NT-induced VEGF mRNA upregulation was completely abolished by HXM (1.03 ± 0.02 in cells treated with NT and HXM versus 1.84 ± 0.27 in cells treated with NT alone; $P < 0.01$), suggesting that the effect of NT 10^{-8} M on VEGF mRNA expression is mediated through activation of nAchR (Fig. 5F). We also showed that NT-induced PEDF mRNA downregulation was completely abolished by HXM (1.02 ± 0.06 in cells treated with NT and HXM versus 0.81 ± 0.02 in cells treated with NT alone; $P < 0.05$; Fig. 5G). These data suggest that the effect of NT on PEDF mRNA expression is mediated by nAchR.

RPE from Rats Constitutively Express the α4, α5, α7, and β2 nAchR Subunits

Aware of advantages and limitations of in vitro studies, including the possibility that the ARPE-19 cell differentiation state may not be similar to adult cells in vivo, we decided to investigate whether our observations on cultured human RPE cells could be confirmed in an animal model. Consistent with our in vitro data, we used real-time PCR to demonstrate the constitutive expression of nAchR subtype transcripts in RPE from rats. As shown in Figure 6A, we found that rat RPE extracts expressed the nAChR α4, α5, α7, and β2 subunits. We did not detect any significant expression of other isoforms. The α4 nAchR subunit was by far the most abundant subtype, as its levels were ~116-fold higher than α5 (116.0 ± 9.2 vs. 1.00 ± 0.14, $P < 0.0001$; Fig. 6B), ~226-fold higher than α7 (226.7 ± 18.0 vs. 1.00 ± 0.15, $P < 0.0001$; Fig. 6C), and ~6.0-fold higher than β2 (6.1 ± 0.5 vs. 1.00 ± 0.11, $P < 0.0001$; Fig. 6D). These findings demonstrate that under basal conditions, rat RPE expresses several subtypes of nAChR that could mediate deleterious cellular responses after activation with NT.

NT Induces α4 nAchR Subtype Transcriptional Activation in RPE from Rats

In this study, exposure to NT increased β1 nAchR subtype mRNA expression in ARPE-19 cells. Based on these observations, we sought to determine whether such transcriptional activation of the predominant nAchR isoform also occurs in vivo. Indeed, α4 nAchR subtype mRNA expression was robustly upregulated by 61% (1.61 ± 0.15 vs. 1.00 ± 0.04; $P < 0.001$) in RPE from rats treated with NT for 3 days relative to controls (Fig. 7). These data confirm our in vitro observations and indicate that prolonged exposure to NT increases the number of α4 nAchR isoforms in rat RPE in vivo.

NT Increases the Ratio between VEGF and PEDF through nAchR in RPE from Rats

In this study, exposure of ARPE-19 cells to NT increased VEGF mRNA and protein levels and concomitantly decreased PEDF mRNA and protein expression, which resulted in an increased VEGF/PEDF protein ratio. To determine whether these effects of NT in vitro in ARPE-19 cells are consistent with changes in

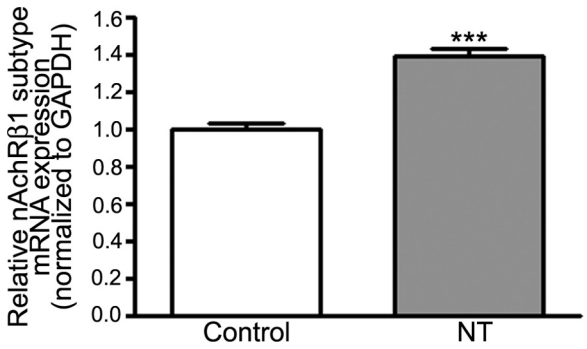

FIGURE 4. NT upregulated the nAchR β1 subtype expression in ARPE-19 cells. Confluent serum-starved ARPE-19 cells were treated with NT 10^{-8} M for 72 hours, and total RNA was extracted to assess nAchR β1 mRNA expression by real-time PCR. *GAPDH* was used as the housekeeping gene. Data are expressed as the mean ± SE and represent the average results of three independent experiments run in duplicate. $^{***}P < 0.0001$ versus control.

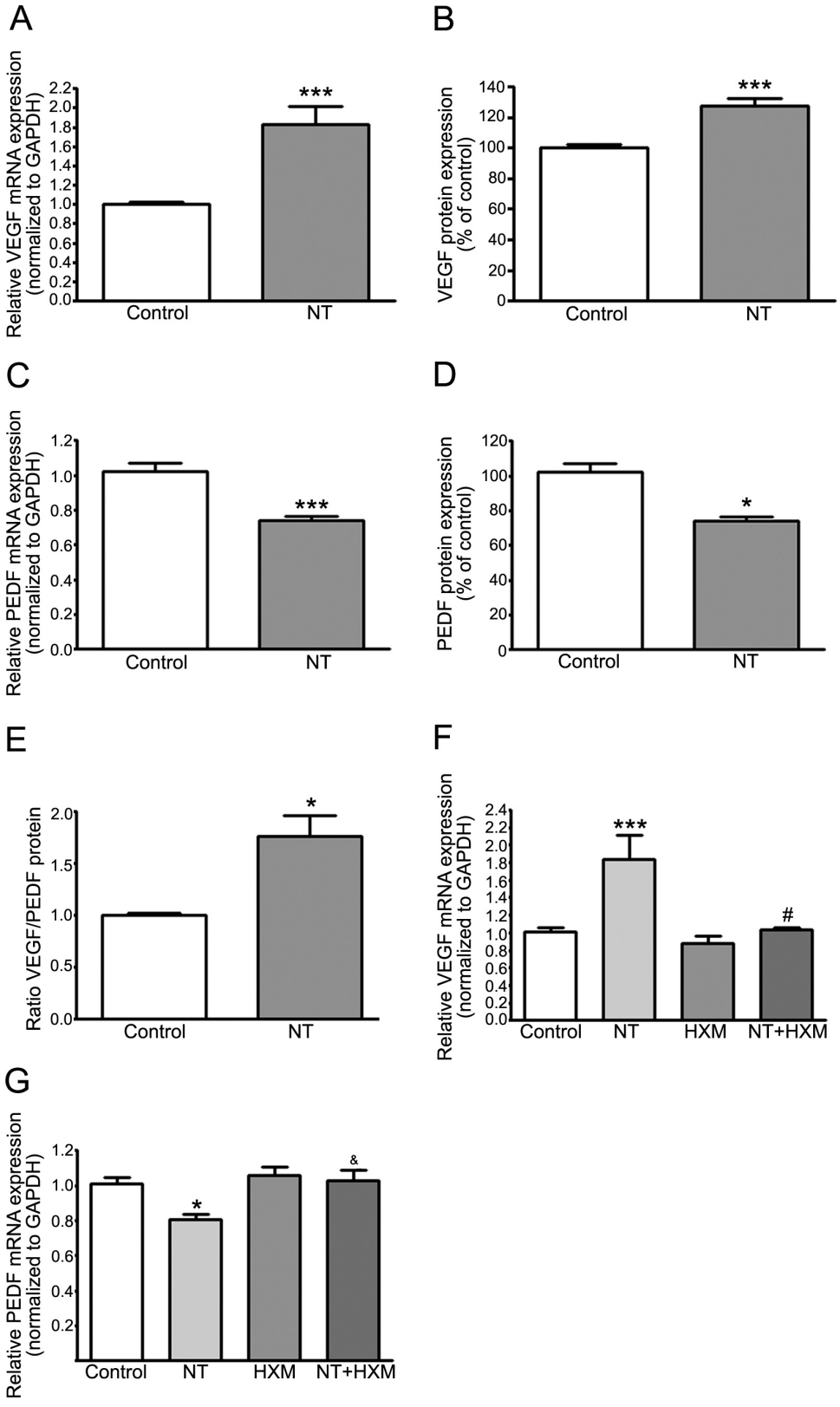

FIGURE 5. NT increased VEGF expression and decreased PEDF expression through nAchR in ARPE-19 cells. NT (**A**) increased VEGF and (**C**) decreased PEDF mRNA expression in ARPE-19 cells. Confluent serum-starved ARPE-19 cells were treated with NT 10^{-8} M for 72 hours. Total RNA was extracted to assess VEGF and PEDF mRNA expression by real-time PCR. *GAPDH* was used as housekeeping gene. NT (**B**) increased VEGF and (**D**) decreased PEDF protein expression. Concentration of VEGF and PEDF secreted in supernatants of confluent serum-starved ARPE-19 cells treated with NT 10^{-8} M for 72 hours was assessed by ELISA. (**E**) NT increased VEGF/PEDF protein ratio. NT-induced (**F**) upregulation of VEGF and (**G**) downregulation of PEDF mRNA expression was abolished by HXM. Confluent serum-starved ARPE-19 cells were preincubated with HXM 10^{-5} M for 1 hour and then exposed to NT 10^{-8} M for 72 hours. Total RNA was extracted to assess VEGF and PEDF mRNA expression by real-time PCR. *GAPDH* was used as housekeeping gene. Data are expressed as the mean ± SE and represent the average results of three to four independent experiments run in duplicate. $^{*}P < 0.05$ and $^{***}P < 0.0001$ versus control; $\#P < 0.01$ and $\&P < 0.05$ versus NT alone.

vivo, we sought evidence for imbalance between VEGF and PEDF in RPE from rats exposed to NT for 3 days. We showed that VEGF mRNA expression was strongly upregulated (~1.2-fold) in rat RPE after exposure to NT relative to control rats (2.16 ± 0.32 vs. 1.04 ± 0.14; $P < 0.01$; Fig. 8A). VEGF protein expression was concomitantly increased by 98% (198.0% ± 12.7% versus 100.0% ± 1.7%; $P < 0.001$) relative to the controls (Fig. 8C). Surprisingly, treatment with NT robustly upregulated PEDF mRNA expression (~2.6-fold) in rat RPE compared with the controls (3.63 ± 0.58 vs. 1.00 ± 0.1; $P < 0.001$; Fig. 8B). However, PEDF protein expression was reduced by 46% compared with that in control rats (54.0% ± 12.7% versus

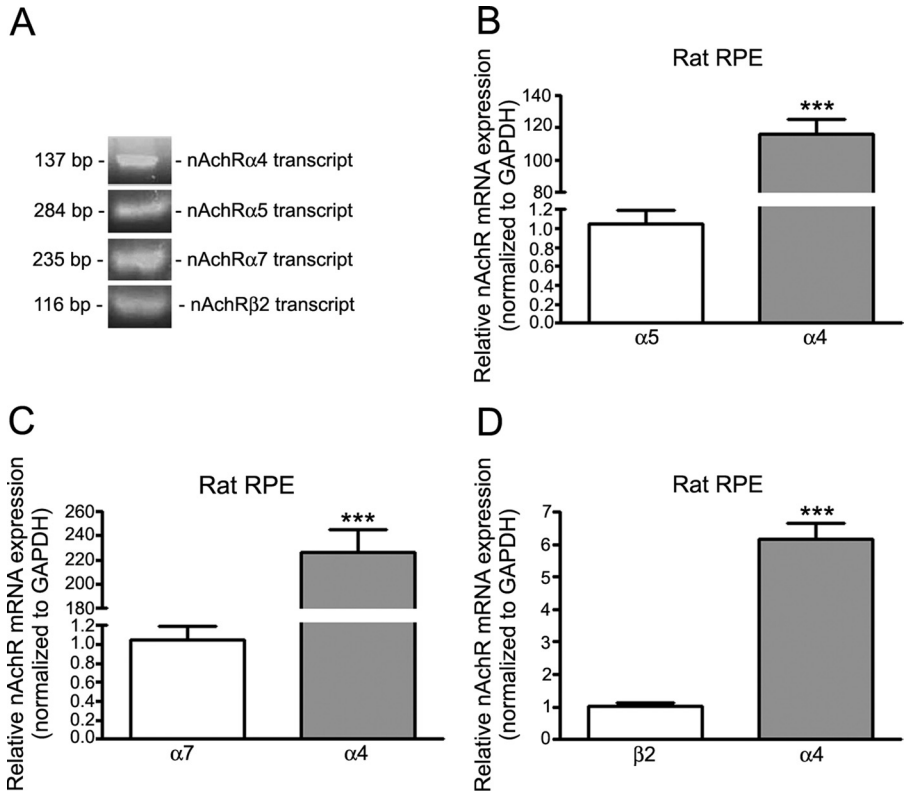

FIGURE 6. RPE from rats constitutively expressed the $\alpha 4$, $\alpha 5$, $\alpha 7$, and $\beta 2$ nAchR subunits. Real-time PCR demonstrated the presence of the nAchR $\alpha 4$, $\alpha 5$, $\alpha 7$, and $\beta 2$ subunit transcripts (**A–D**) and the prevalence of the $\alpha 4$ subtype (**B–D**) in RPE from Sprague-Dawley rats (pooled RNA from five rats/lane). Real-time PCR for $\alpha 4$, $\alpha 5$, $\alpha 7$, and the $\beta 2$ nAchR isoforms was followed by ethidium bromide-stained agarose gel electrophoresis to visualize the products (**A**). Shown are representative gels. Shown on the *left* is the size of the transcripts base pairs. $^{***}P < 0.0001$.

100.0% ± 1.6, $P < 0.05$; Fig. 8D). In ARPE-19 cells, we showed that prolonged exposure to NT increased the VEGF/PEDF protein ratio by ~2.4-fold in rat RPE (3.40 ± 0.34 vs. 1.00 ± 0.11, $P < 0.01$; Fig. 8E). Consistent with our in vitro observations, we also showed that NT-induced VEGF mRNA upregulation was almost completely abolished by HXM (1.20 ± 0.15 vs. 2.16 ± 0.32; $P < 0.05$; Fig. 8A). Furthermore, HXM inhibited by 35.5% the increase in PEDF mRNA resulting from exposure to NT (2.34 ± 0.17 vs. 3.63 ± 0.58; $P < 0.05$; Fig. 8B). These results suggest that the effect of NT on VEGF and PEDF transcriptional activation is nAchR mediated.

DISCUSSION

Herein, we performed studies aimed at elucidating potential mechanisms by which NT in concentrations similar to those achieved in the plasma of passive smokers may induce pathologic angiogenesis and accelerate the progression of AMD to the blinding wet form of the disease. We demonstrated for the first time the presence of functionally active nAchRs that contain the $\alpha 3$, $\alpha 10$ and $\beta 1$ subunits in cultured human RPE cells and the $\alpha 4$, $\alpha 5$, $\alpha 7$, and $\beta 2$ subtypes in RPE from rats. We also established that the $\beta 1$ and $\alpha 4$ were the predominant isoforms in RPE cells and RPE from rats, respectively. In addition, we showed that exposure to NT at clinically relevant concentrations representative of those seen in the plasma of passive smokers resulted in transcriptional activation of the nAchR $\beta 1$ and $\alpha 4$ subtypes and nAchR-mediated disruption of the normal balance between RPE-derived VEGF and PEDF resulting in increased VEGF-to-PEDF ratio in ARPE-19 cells and RPE from rats. Under these conditions, NT did not show any lethal or proliferative effect on RPE.

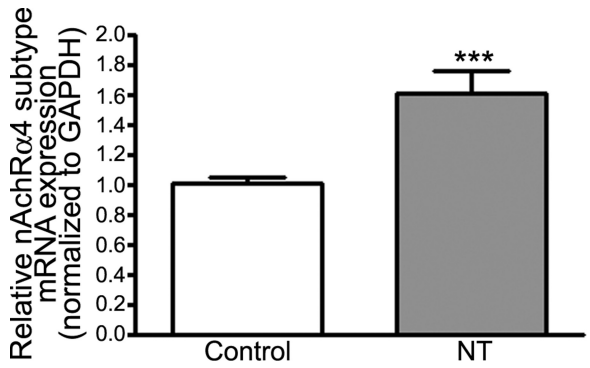

FIGURE 7. NT upregulated nAchR $\alpha 4$ subtype expression in rat RPE. Total RNA was extracted from RPE microdissected from Sprague-Dawley rats treated with NT (100 μg/mL) in drinking water for 3 days. The expression of nAchR $\alpha 4$ mRNA was assessed by real-time PCR using *GAPDH* as housekeeping gene (pooled RNA from five rats/lane). Data are expressed as a percentage of control and are the mean ± SE. $^{***}P < 0.0001$ versus control.

NT exerts its cellular functions through nAChRs comprising a combinatorial association of α and β subunits.[34,35] nAchRs are expressed in a wide variety of peripheral non-neuronal, nonexcitable cells including hepatocytes,[36] skin keratinocytes,[37] bronchial epithelial cells,[38] vascular smooth muscle cells,[39] peripheral blood mononuclear cells,[40] mesangial cells,[44] and vascular, retinal and choroidal endothelial cells,[41–43] suggesting that these receptors have distinct functions well beyond neurotransmission. nAchR expression has also been characterized in rat retina.[67] However, it is not known whether and which type of nAchR is expressed in RPE cells. In this study, we report for the first time that ARPE-19 cells constitutively expressed functionally active nAchR containing the $\alpha 3$, $\alpha 10$, and $\beta 1$ subunits, with $\beta 1$ being the most abundant isoform. These results were subsequently confirmed in human primary cells generated and characterized in our laboratory. The ARPE-19 is a nontransformed human RPE cell line with normal karyology[55] that is routinely used as an alternative to primary cultures because of its ready availability and the stability of its features in prolonged cultivation. ARPE-19 cells retain many of the characteristics of RPE cells, including cell morphology and functional tight junctions[55] and

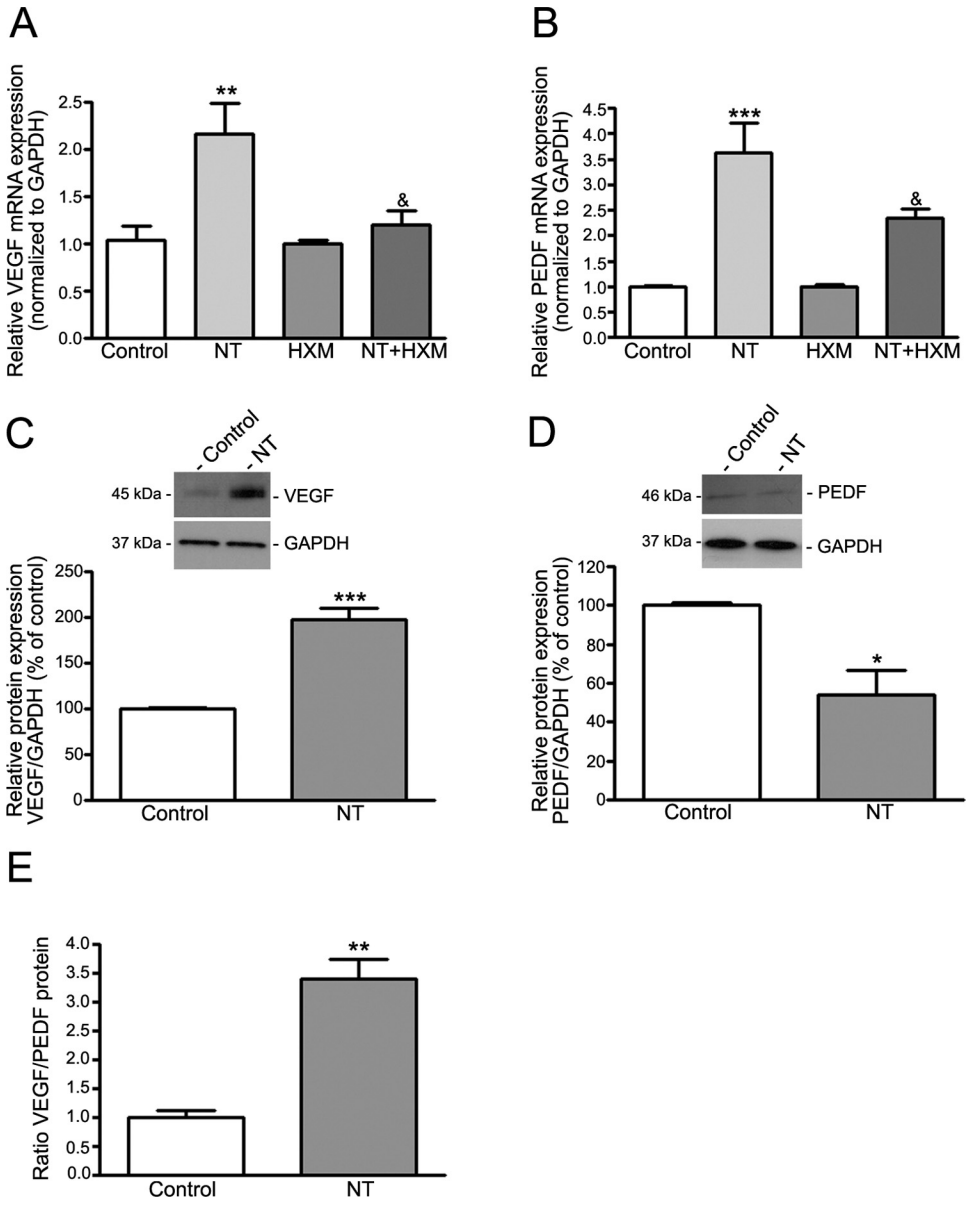

FIGURE 8. NT increased VEGF expression and decreased PEDF protein expression through nAchR in rat RPE. NT (**A**) increased VEGF and (**B**) PEDF mRNA expression in rat RPE. (**A**) NT-increased VEGF and (**B**) PEDF mRNA expression was abolished by HXM. Total RNA was extracted from RPE microdissected from Sprague-Dawley rats treated with NT (100 μg/mL) in drinking water for 3 days, with or without intraperitoneal injections of nonspecific nicotinic antagonist HXM (40 mg/kg/d) for 3 days. VEGF and PEDF mRNA expression was assessed by real-time PCR using *GAPDH* as housekeeping gene (pooled RNA from five rats/lane). NT (**C**) increased VEGF and (**D**) decreased PEDF protein expression in rat RPE. (**E**) NT increased the VEGF/PEDF protein ratio. Total protein was extracted from RPE microdissected from Sprague-Dawley rats treated with NT (100 μg/mL) in drinking water for 3 days. VEGF, PEDF, and GAPDH protein expression was assessed by Western blot analysis (pooled protein from five rats/lane). GAPDH served as the loading control. (**C**, **D**) *Top*: representative Western blot. The protein's molecular mass is shown on the *left* in kilodaltons (kDa). *Bottom*: average densitometry results. Data are expressed as a percentage of control and are the mean ± SE. $^{*}P < 0.05$, $^{**}P < 0$ 01, $^{***}P < 0.0001$ versus control; $\&P < 0.05$ versus NT alone.

the ability to phagocytose rod outer segments.[68] They also express the RPE-specific markers CRALBP and RPE65.[55] However, the limitations associated with the use of an established cell line like ARPE-19 cells include potential phenotypic changes after multiple passages as well as the possibility that ARPE-19 cells may represent only a subset of primary RPE cells. In addition, ARPE-19 cells and human primary RPE cells may respond differently with respect to certain functional properties due to differences in protein profiling.[69,70] On the other hand, ARPE-19 cells overcome some of the limitations imposed by primary human RPE cell cultures that require donor eyes with a short postmortem time. In addition, primary cultures of human RPE cells exhibit phenotypic differences in vitro[71] and may present other physiological differences caused by donor-to-donor variabilities. In fact, these authors identified eight discrete phenotypes of RPE cells within the same cultures. Keeping all this in mind, the similarities we report in the expression pattern of nAchR prompted us to perform all subsequent experiments in ARPE-19 cells. Aware of advantages and limitations of in vitro studies, including the possibility that the ARPE-19 cell differentiation state may not be not similar to adult cells in vivo, our initial in vitro observations were later confirmed in an animal model showing that the nAchR $\alpha 4$, $\alpha 5$, $\alpha 7$, and $\beta 2$ isotypes are expressed in rat RPE. Furthermore, we identified $\beta 1$ and $\alpha 4$ as the prevalent isoforms in RPE cells and rat RPE, respectively. These results strongly suggest that NT signals directly through these receptors in the RPE which may have important functional roles relevant to pathologic angiogenesis. Therefore, it is reasonable to assume that the harmful role that NT may play in the pathogenesis of AMD may be mediated, at least in part, through its direct nAchR-mediated deleterious effects on RPE cells.

Cell proliferation is the underlying cause of a wide variety of diseases. NT has been shown to induce proliferation through its nAchR in endothelial cells,[32,33,43] which lies at the origin of angiogenesis. Previous work from our group has demonstrated that NT 10^{-8} M for 24 hours did not induce any cell growth in a primary cell line of choroidal vascular smooth muscle cells isolated from C57BL/6 mice, as determined by cell count.[45] As reported here, we did not observe any proliferation of RPE cells resulting from exposure to NT for 72 hours at pathophysiologically relevant concentrations in this study either. Previous studies described no significant alteration of either proliferation of primary RPE cells in response to NT treatment for 3 days[72] or cell viability of ARPE-19 cells after exposure to NT for

24 hours.[73] Our results are a confirmation of these observations. However, it is worth noting that the concentrations were very high (10^{-6} and 0.5×10^{-6} M)[72] and even nonphysiological (10^{-2} and 10^{-4} M)[73] compared with the dose we elected to use in the present study. According to our data, it is likely that the harmful proangiogenic actions of NT on RPE cells are not mediated through abnormal effects on cell growth.

Upregulation in brain nAChR has been widely described after chronic treatment with NT.[64] Our study demonstrated for the first time that exposure of RPE to NT for 72 hours at concentrations representative of those seen in the plasma of passive smokers led to increased mRNA levels of the predominant $\beta 1$ and $\alpha 4$ nAChR isoforms. These findings demonstrate that NT can rapidly transcriptionally modulate the expression of prevalent nAChR subtypes in vitro and in vivo and therefore increase the number of NT binding sites in RPE, which may have important implications for the harmful proangiogenic effects of NT.

Multiple lines of evidence show that NT activates several mitogen-activated protein kinase signaling cascades in a variety of tissues and cell types.[74–76] In the present study, we sought to evaluate the ERK1/2 pathway to verify the functionality of nAChR expressed in RPE cells. We found that stimulation of ARPE-19 cells with NT led to a robust and rapid induction of ERK1/2 phosphorylation that was completely blocked by HXM, a nonselective antagonist of nAchR. To our knowledge, there has been no reported study in the literature describing the effects of NT on the ERK1/2 signaling pathway in human RPE cells. However, our results are consistent with previous studies on various non-neuronal and neuronal systems that have described an activation of the *ERK1/2* cascade in response to NT.[63,75,77,78] Thus, our data confirm that NT exerts its biological effects by binding to nAchR leading to *ERK*1/2 regulation in RPE cells, which could be involved in the proangiogenic effects of NT.

In normal tissues, angiogenic homeostasis is controlled by a delicate balance between pro- and antiangiogenic factors.[79] CNV-related angiogenesis requires both an alteration in the concentration of molecules that stimulate or inhibit growth of new blood vessels.[7] VEGF plays a key role in angiogenesis by regulating endothelial cells proliferation, migration, and survival.[80] Of interest, secretion of VEGF by RPE cells is polarized, as the basal secretion toward Bruch's membrane is two to seven times higher than the apical secretion toward the photoreceptors.[81] This disparity is of particular biological significance for the proangiogenic effects of NT, due to the close proximity of Bruch's membrane to the endothelial cells of the choriocapillaries. Increased VEGF expression has been reported in surgically excised AMD-associated choroidal neovascular membranes.[82,83] Previous studies have shown that NT upregulates VEGF expression in endothelial[48] and vascular smooth muscle cells.[63] Moreover, exposure of mice to second-hand smoke, which contains the highest concentrations of NT, has been shown to increase plasma levels of VEGF.[84] PEDF, which functions as an antiangiogenic factor that inhibits endothelial cells proliferation and stabilizes the endothelium of the choriocapillaries,[15,85] counterbalances the effect of VEGF and modulates the formation of CNV.[65,66] A decrease in PEDF expression has been reported in eyes with AMD, therefore disrupting the critical balance between VEGF and PEDF that may be permissive of the development of CNV.[66] In our study, exposure of ARPE-19 cells to NT increased VEGF and decreased PEDF expression, leading to a ~1.8 VEGF/PEDF protein ratio, which may promote angiogenesis. Indeed, Gao et al.[86] reported that retinas from rats with ischemia-induced neovascularization showed a fivefold increase in VEGF levels and a twofold decrease in PEDF expression compared with the controls, resulting in an increase in the VEGF/PEDF ratio to 2.5.[86] Our in vitro observations were further corroborated in vivo by the finding of a robust ~2.4-fold increase in VEGF-to-PEDF protein ratio in RPE from rats after exposure to NT. Of note, we found that NT upregulated PEDF mRNA expression while downregulating PEDF protein expression. It can be hypothesized that posttranscriptional regulatory mechanisms primarily involving PEDF mRNA stability explains the decreased PEDF protein expression in rat RPE. The reasons for the difference between in vitro and in vivo observations regarding the regulation of PEDF mRNA in response to NT are not clear but may be explained by the fact that the mammalian organism's milieu and a fully formed organ like the retina constitute an exponentially more complex system than do isolated RPE cells in culture. Species difference between human RPE cells and rats may also account for the discrepancy in results. VEGF and PEDF transcriptional activation induced by NT was almost completely abolished by nonspecific nAchR antagonist HXM, both in vitro and in vivo. These results demonstrate that the proangiogenic effects of NT are mediated through nAchR and provide direct support for a key contribution of RPE cells to NT-stimulated angiogenesis. Given that there is currently no specific antagonist of $\beta 1$ nAchR subtype commercially available, we have not been able to investigate whether this particular isoform which is the most abundant in cultured human RPE cells, is the one mediating NT-induced effects on VEGF and PEDF expression. Additional studies using siRNA that targets the $\beta 1$ nAchR subtype are needed, to clarify the contribution of this isoform to the proangiogenic effects of NT in RPE cells.

In summary, our results demonstrate an important contribution of RPE cells to the proangiogenic effects of NT. Our data provide evidence that NT has a direct effect on the RPE through its nAchR. The increase in VEGF/PEDF ratio induced by NT may play a key role in CNV-related angiogenesis in AMD patients who are passive smokers.

Acknowledgments

The authors thank Eleut Hernandez and Omer Alomari for technical support.

References

1. Augood CA, Vingerling JR, de Jong PT, et al. Prevalence of age-related maculopathy in older Europeans: the European Eye Study (EUREYE). *Arch Ophthalmol.* 2006;124:529–535.
2. Evans JR. Risk factors for age-related macular degeneration. *Prog Retin Eye Res.* 2001;20:227–253.
3. Javitt JC, Zhou Z, Maguire MG, Fine SL, Willke RJ. Incidence of exudative age-related macular degeneration among elderly Americans. *Ophthalmology.* 2003;110:1534–1539.
4. Klein R, Peto T, Bird A, Vannewkirk MR. The epidemiology of age-related macular degeneration. *Am J Ophthalmol.* 2004;137:486–495.
5. Rein DB, Wittenborn JS, Zhang X, Honeycutt AA, Lesesne SB, Saaddine J. Forecasting age-related macular degeneration through the year 2050: the potential impact of new treatments. *Arch Ophthalmol.* 2009;127:533–540.
6. Green WR. Histopathology of age-related macular degeneration. *Mol Vis.* 1999;5:27.
7. Ohno-Matsui K, Morita I, Tombran-Tink J, et al. Novel mechanism for age-related macular degeneration: an equilibrium shift between the angiogenesis factors VEGF and PEDF. *J Cell Physiol.* 2001;189:323–333.
8. Kwak N, Okamoto N, Wood JM, Campochiaro PA. VEGF is major stimulator in model of choroidal neovascularization. *Invest Ophthalmol Vis Sci.* 2000;41:3158–3164.
9. Husain D, Ambati B, Adamis AP, Miller JW. Mechanisms of age-related macular degeneration. *Ophthalmol Clin North Am.* 2002;15:87–91.

10. Witmer AN, Vrensen GF, Van Noorden CJ, Schlingemann RO. Vascular endothelial growth factors and angiogenesis in eye disease. *Prog Retin Eye Res.* 2003;22:1–29.
11. Tombran-Tink J, Barnstable CJ. Therapeutic prospects for PEDF: more than a promising angiogenesis inhibitor. *Trends Mol Med.* 2003;9:244–250.
12. Bouck N. PEDF: anti-angiogenic guardian of ocular function. *Trends Mol Med.* 2002;8:330–334.
13. Young RW. Pathophysiology of age-related macular degeneration. *Surv Ophthalmol.* 1987;31:291–306.
14. Adamis AP, Shima DT, Yeo KT, et al. Synthesis and secretion of vascular permeability factor/vascular endothelial growth factor by human retinal pigment epithelial cells. *Biochem Biophys Res Commun.* 1993;193:631–638.
15. Dawson DW, Volpert OV, Gillis P, et al. Pigment epithelium-derived factor: a potent inhibitor of angiogenesis. *Science.* 1999; 285:245–248.
16. Tong JP, Yao YF. Contribution of VEGF and PEDF to choroidal angiogenesis: a need for balanced expressions. *Clin Biochem.* 2006;39:267–276.
17. Katta S, Kaur I, Chakrabarti S. The molecular genetic basis of age-related macular degeneration: an overview. *J Genet.* 2009;88: 425–449.
18. Christen WG, Glynn RJ, Manson JE, Ajani UA, Buring JE. A prospective study of cigarette smoking and risk of age-related macular degeneration in men. *JAMA.* 1996;276:1147–1151.
19. Seddon JM, Willett WC, Speizer FE, Hankinson SE. A prospective study of cigarette smoking and age-related macular degeneration in women. *JAMA.* 1996;276:1141–1146.
20. Klein R, Klein BE, Moss SE. Relation of smoking to the incidence of age-related maculopathy. The Beaver Dam Eye Study. *Am J Epidemiol.* 1998;147:103–110.
21. Solberg Y, Rosner M, Belkin M. The association between cigarette smoking and ocular diseases. *Surv Ophthalmol.* 1998;42:535–547.
22. Smith W, Mitchell P, Leeder SR. Smoking and age-related maculopathy. The Blue Mountains Eye Study. *Arch Ophthalmol.* 1996; 114:1518–1523.
23. Klein R, Klein BE, Linton KL, DeMets DL. The Beaver Dam Eye Study: the relation of age-related maculopathy to smoking. *Am J Epidemiol.* 1993;137:190–200.
24. Tamakoshi A, Yuzawa M, Matsui M, Uyama M, Fujiwara NK, Ohno Y. Smoking and neovascular form of age related macular degeneration in late middle aged males: findings from a case-control study in Japan. Research Committee on Chorioretinal Degenerations. *Br J Ophthalmol.* 1997;81:901–904.
25. Delcourt C, Diaz JL, Ponton-Sanchez A, Papoz L. Smoking and age-related macular degeneration. The POLA Study. Pathologies Oculaires Liees a l'Age. *Arch Ophthalmol.* 1998;116:1031–1035.
26. Thornton J, Edwards R, Mitchell P, Harrison RA, Buchan I, Kelly SP. Smoking and age-related macular degeneration: a review of association. *Eye (Lond).* 2005;19:935–944.
27. Klein R, Knudtson MD, Cruickshanks KJ, Klein BE. Further observations on the association between smoking and the long-term incidence and progression of age-related macular degeneration: the Beaver Dam Eye Study. *Arch Ophthalmol.* 2008;126:115–121.
28. Khan JC, Thurlby DA, Shahid H, et al. Smoking and age related macular degeneration: the number of pack years of cigarette smoking is a major determinant of risk for both geographic atrophy and choroidal neovascularisation. *Br J Ophthalmol.* 2006;90:75–80.
29. Lois N, Abdelkader E, Reglitz K, Garden C, Ayres JG. Environmental tobacco smoke exposure and eye disease. *Br J Ophthalmol.* 2008;92:1304–1310.
30. Hammond SK. Exposure of U.S. workers to environmental tobacco smoke. Environ *Health Perspect*. 1999;107(suppl 2):329–340.
31. Okoli CT, Kelly T, Hahn EJ. Secondhand smoke and nicotine exposure: a brief review. *Addict Behav.* 2007;32:1977–1988.
32. Heeschen C, Jang JJ, Weis M, et al. Nicotine stimulates angiogenesis and promotes tumor growth and atherosclerosis. *Nat Med.* 2001;7:833–839.
33. Villablanca AC. Nicotine stimulates DNA synthesis and proliferation in vascular endothelial cells in vitro. *J Appl Physiol.* 1998;84: 2089–2098.
34. Sharma G, Vijayaraghavan S. Nicotinic receptor signaling in non-excitable cells. *J Neurobiol.* 2002;53:524–534.
35. Leonard S, Bertrand D. Neuronal nicotinic receptors: from structure to function. *Nicotine Tob Res.* 2001;3:203–223.
36. Dewar BJ, Bradford BU, Thurman RG. Nicotine increases hepatic oxygen uptake in the isolated perfused rat liver by inhibiting glycolysis. *J Pharmacol Exp Ther.* 2002;301:930–937.
37. Grando SA, Horton RM, Pereira EF, et al. A nicotinic acetylcholine receptor regulating cell adhesion and motility is expressed in human keratinocytes. *J Invest Dermatol.* 1995;105:774–781.
38. Maus AD, Pereira EF, Karachunski PI, et al. Human and rodent bronchial epithelial cells express functional nicotinic acetylcholine receptors. *Mol Pharmacol.* 1998;54:779–788.
39. Carty CS, Huribal M, Marsan BU, Ricotta JJ, Dryjski M. Nicotine and its metabolite cotinine are mitogenic for human vascular smooth muscle cells. *J Vasc Surg.* 1997;25:682–688.
40. Wongsriraksa A, Parsons ME, Whelan CJ. Characterisation of nicotine receptors on human peripheral blood mononuclear cells (PBMC). *Inflamm Res.* 2009;58:38–44.
41. Kiuchi K, Matsuoka M, Wu JC, et al. Mecamylamine suppresses basal and nicotine-stimulated choroidal neovascularization. *Invest Ophthalmol Vis Sci.* 2008;49:1705–1711.
42. Macklin KD, Maus AD, Pereira EF, Albuquerque EX, Conti-Fine BM. Human vascular endothelial cells express functional nicotinic acetylcholine receptors. *J Pharmacol Exp Ther.* 1998;287:435–439.
43. Heeschen C, Weis M, Aicher A, Dimmeler S, Cooke JP. A novel angiogenic pathway mediated by non-neuronal nicotinic acetylcholine receptors. *J Clin Invest.* 2002;110:527–536.
44. Jaimes EA, Tian RX, Raij L. Nicotine: the link between cigarette smoking and the progression of renal injury? *Am J Physiol Heart Circ Physiol.* 2007;292:H76−H82.
45. Suner IJ, Espinosa-Heidmann DG, Marin-Castano ME, Hernandez EP, Pereira-Simon S, Cousins SW. Nicotine increases size and severity of experimental choroidal neovascularization. *Invest Ophthalmol Vis Sci.* 2004;45:311–317.
46. Dom AM, Buckley AW, Brown KC, et al. The α7-nicotinic acetylcholine receptor and MMP-2/9 pathway mediate the pro-angiogenic effect of nicotine in human retinal endothelial cells. *Invest Ophthalmol Vis Sci*. Published online June 16, 2010.
47. Egleton RD, Brown KC, Dasgupta P. Angiogenic activity of nicotinic acetylcholine receptors: implications in tobacco-related vascular diseases. *Pharmacol Ther.* 2009;121:205–223.
48. Conklin BS, Zhao W, Zhong DS, Chen C. Nicotine and cotinine up-regulate vascular endothelial growth factor expression in endothelial cells. *Am J Pathol.* 2002;160:413–418.
49. Espinosa-Heidmann DG, Suner IJ, Catanuto P, Hernandez EP, Marin-Castano ME, Cousins SW. Cigarette smoke-related oxidants and the development of sub-RPE deposits in an experimental animal model of dry AMD. *Invest Ophthalmol Vis Sci.* 2006;47: 729–737.
50. Marin-Castano ME, Striker GE, Alcazar O, Catanuto P, Espinosa-Heidmann DG, Cousins SW. Repetitive nonlethal oxidant injury to retinal pigment epithelium decreased extracellular matrix turnover in vitro and induced sub-RPE deposits in vivo. *Invest Ophthalmol Vis Sci.* 2006;47:4098–4112.
51. Marin-Castano ME, Csaky KG, Cousins SW. Nonlethal oxidant injury to human retinal pigment epithelium cells causes cell membrane blebbing but decreased MMP-2 activity. *Invest Ophthalmol Vis Sci.* 2005;46:3331–3340.
52. Strunnikova N, Zhang C, Teichberg D, et al. Survival of retinal pigment epithelium after exposure to prolonged oxidative injury: a detailed gene expression and cellular analysis. *Invest Ophthalmol Vis Sci.* 2004;45:3767–3777.
53. Bertram KM, Baglole CJ, Phipps RP, Libby RT. Molecular regulation of cigarette smoke induced-oxidative stress in human retinal pigment epithelial cells: implications for age-related macular degeneration. *Am J Physiol Cell Physiol.* 2009;297:C1200–C1210.
54. Wang AL, Lukas TJ, Yuan M, Du N, Handa JT, Neufeld AH. Changes in retinal pigment epithelium related to cigarette smoke: possible relevance to smoking as a risk factor for age-related macular degeneration. *PLoS One.* 2009;4:e5304.

55. Dunn KC, Aotaki-Keen AE, Putkey FR, Hjelmeland LM. ARPE-19, a human retinal pigment epithelial cell line with differentiated properties. *Exp Eye Res.* 1996;62:155–169.
56. Calafat AM, Polzin GM, Saylor J, Richter P, Ashley DL, Watson CH. Determination of tar, nicotine, and carbon monoxide yields in the mainstream smoke of selected international cigarettes. *Tob Control.* 2004;13:45–51.
57. Vandesompele J, De Preter K, Pattyn F, et al. Accurate normalization of real-time quantitative RT-PCR data by geometric averaging of multiple internal control genes. *Genome Biol.* 2002;3:RESEARCH0034.
58. Malfitano C, Alba Loureiro TC, Rodrigues B, et al. Hyperglycaemia protects the heart after myocardial infarction: aspects of programmed cell survival and cell death. *Eur J Heart Fail* 12:659–667.
59. Zhu D, Xu X, Zheng Z, Gu Q. Regulation of vascular endothelial growth factor and pigment epithelium-derived factor in rat retinal explants under retinal acidification. *Eye* (*Lond*). 2009;23:2105–2111.
60. Mikulski Z, Hartmann P, Jositsch G, et al. Nicotinic receptors on rat alveolar macrophages dampen ATP-induced increase in cytosolic calcium concentration. *Respir Res*. 11:133.
61. Livak KJ, Schmittgen TD. Analysis of relative gene expression data using real-time quantitative PCR and the 2(−Delta Delta C(T)) method. *Methods.* 2001;25:402–408.
62. Benowitz NL, Kuyt F, Jacob P 3rd. Influence of nicotine on cardiovascular and hormonal effects of cigarette smoking. *Clin Pharmacol Ther*. 1984;36:74−81.
63. Kanda Y, Watanabe Y. Nicotine-induced vascular endothelial growth factor release via the EGFR-ERK pathway in rat vascular smooth muscle cells. *Life Sci.* 2007;80:1409–1414.
64. Mochizuki T, Villemagne VL, Scheffel U, et al. Nicotine induced up-regulation of nicotinic receptors in CD-1 mice demonstrated with an in vivo radiotracer: gender differences. *Synapse.* 1998;30:116–118.
65. Ogata N, Wada M, Otsuji T, Jo N, Tombran-Tink J, Matsumura M. Expression of pigment epithelium-derived factor in normal adult rat eye and experimental choroidal neovascularization. *Invest Ophthalmol Vis Sci.* 2002;43:1168–1175.
66. Bhutto IA, McLeod DS, Hasegawa T, et al. Pigment epithelium-derived factor (PEDF) and vascular endothelial growth factor (VEGF) in aged human choroid and eyes with age-related macular degeneration. *Exp Eye Res.* 2006;82:99–110.
67. Moretti M, Vailati S, Zoli M, et al. Nicotinic acetylcholine receptor subtypes expression during rat retina development and their regulation by visual experience. *Mol Pharmacol.* 2004;66:85–96.
68. Finnemann SC, Bonilha VL, Marmorstein AD, Rodriguez-Boulan E. Phagocytosis of rod outer segments by retinal pigment epithelial cells requires alpha(v)beta5 integrin for binding but not for internalization. *Proc Natl Acad Sci U S A.* 1997;94:12932–12937.
69. Alge CS, Hauck SM, Priglinger SG, Kampik A, Ueffing M. Differential protein profiling of primary versus immortalized human RPE cells identifies expression patterns associated with cytoskeletal remodeling and cell survival. *J Proteome Res.* 2006;5:862−878.
70. Proulx S, Landreville S, Guerin SL, Salesse C. Integrin alpha5 expression by the ARPE-19 cell line: comparison with primary RPE cultures and effect of growth medium on the alpha5 gene promoter strength. *Exp Eye Res.* 2004;79:157–165.
71. Burke JM, Skumatz CM, Irving PE, McKay BS. Phenotypic heterogeneity of retinal pigment epithelial cells in vitro and in situ. *Exp Eye Res.* 1996;62:63–73.
72. Yang L, Gong H, Wang Y, Yin H, Chen P, Zhang H. Nicotine alters morphology and function of retinal pigment epithelial cells in mice. *Toxicol Pathol*. 2010;38:560–567.
73. Patil AJ, Gramajo AL, Sharma A, Seigel GM, Kuppermann BD, Kenney MC. Differential effects of nicotine on retinal and vascular cells in vitro. *Toxicology.* 2009;259:69–76.
74. Ueno H, Pradhan S, Schlessel D, Hirasawa H, Sumpio BE. Nicotine enhances human vascular endothelial cell expression of ICAM-1 and VCAM-1 via protein kinase C, p38 mitogen-activated protein kinase, NF-kappaB, and AP-1. *Cardiovasc Toxicol.* 2006;6:39–50.
75. Tsai JR, Chong IW, Chen CC, Lin SR, Sheu CC, Hwang JJ. Mitogen-activated protein kinase pathway was significantly activated in human bronchial epithelial cells by nicotine. *DNA Cell Biol.* 2006;25:312–322.
76. Li JM, Cui TX, Shiuchi T, et al. Nicotine enhances angiotensin II-induced mitogenic response in vascular smooth muscle cells and fibroblasts. *Arterioscler Thromb Vasc Biol.* 2004;24:80−84.
77. Steiner RC, Heath CJ, Picciotto MR. Nicotine-induced phosphorylation of ERK in mouse primary cortical neurons: evidence for involvement of glutamatergic signaling and CaMKII. *J Neurochem.* 2007;103:666–678.
78. Toborek M, Son KW, Pudelko A, King-Pospisil K, Wylegala E, Malecki A. ERK 1/2 signaling pathway is involved in nicotine-mediated neuroprotection in spinal cord neurons. *J Cell Biochem.* 2007;100:279–292.
79. Folkman J. Seminars in Medicine of the Beth Israel Hospital, Boston. Clinical applications of research on angiogenesis. *N Engl J Med.* 1995;333:1757–1763.
80. Olsson AK, Dimberg A, Kreuger J, Claesson-Welsh L. VEGF receptor signalling: in control of vascular function. *Nat Rev Mol Cell Biol.* 2006;7:359–371.
81. Blaauwgeers HG, Holtkamp GM, Rutten H, et al. Polarized vascular endothelial growth factor secretion by human retinal pigment epithelium and localization of vascular endothelial growth factor receptors on the inner choriocapillaris: evidence for a trophic paracrine relation. *Am J Pathol.* 1999;155:421–428.
82. Lopez PF, Sippy BD, Lambert HM, Thach AB, Hinton DR. Transdifferentiated retinal pigment epithelial cells are immunoreactive for vascular endothelial growth factor in surgically excised age-related macular degeneration-related choroidal neovascular membranes. *Invest Ophthalmol Vis Sci.* 1996;37:855−868.
83. Kliffen M, Sharma HS, Mooy CM, Kerkvliet S, de Jong PT. Increased expression of angiogenic growth factors in age-related maculopathy. *Br J Ophthalmol.* 1997;81:154–162.
84. Zhu BQ, Heeschen C, Sievers RE, et al. Second hand smoke stimulates tumor angiogenesis and growth. *Cancer Cell.* 2003;4:191–196.
85. King GL, Suzuma K. Pigment-epithelium-derived factor: a key coordinator of retinal neuronal and vascular functions. *N Engl J Med.* 2000;342:349–351.
86. Gao G, Li Y, Zhang D, Gee S, Crosson C, Ma J. Unbalanced expression of VEGF and PEDF in ischemia-induced retinal neovascularization. *FEBS Lett.* 2001;489:270–276.